

Stabilization Strategies for Linear Minigastrin Analogues: Further Improvements *via* the Inclusion of Proline into the Peptide Sequence

Maximilian Klingler, Anton A. Hörmann, Christine Rangger, Laurence Desrues, Hélène Castel, Pierrick Gandolfo, and Elisabeth von Guggenberg*



Cite This: *J. Med. Chem.* 2020, 63, 14668–14679



Read Online

ACCESS |



Metrics & More

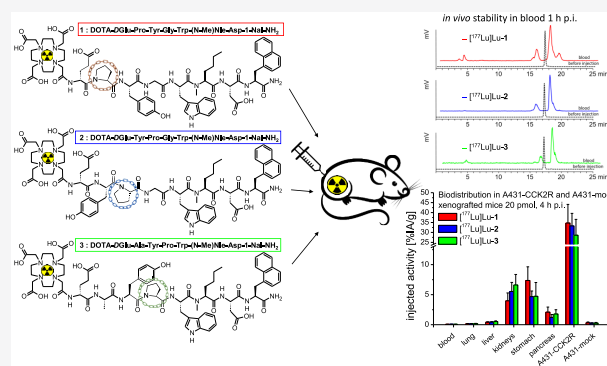


Article Recommendations



Supporting Information

ABSTRACT: Minigastrin (MG) analogues, known for their high potential to target cholecystokinin-2 receptor (CCK2R) expressing tumors, have limited clinical applicability due to low enzymatic stability. By introducing site-specific substitutions within the C-terminal receptor-binding sequence, reduced metabolization and improved tumor targeting can be achieved. In this work, the influence of additional modification within the N-terminal sequence has been explored. Three novel 1,4,7,10-tetraazacyclododecane-1,4,7,10-tetraacetic acid (DOTA)-conjugated CCK2R ligands with proline substitution at different positions were synthesized. Substitution did not affect CCK2R affinity, and the conjugates labeled with indium-111 and lutetium-177 showed a high enzymatic stability in different incubation media as well as *in vivo* (57–79% intact radiopeptide in blood of BALB/c mice at 1 h p.i.) combined with enhanced tumor uptake (29–46% IA/g at 4 h in xenografted BALB/c nude mice). The inclusion of Pro contributes significantly to the development of CCK2R ligands with optimal targeting properties for application in targeted radiotherapy.



INTRODUCTION

Specific targeting of cholecystokinin-2 receptors (CCK2R) for molecular imaging and targeted therapy with radiolabeled peptide derivatives shows a high potential to improve the clinical management of CCK2R-related malignancies. The development of different CCK2R-targeting peptide derivatives was particularly directed toward improving the diagnosis and therapy of medullary thyroid carcinoma (MTC).^{1,2} In addition, the application could be extended also to other tumor entities, such as small cell lung cancer, astrocytoma, stromal ovarian cancer, gastrointestinal stromal tumors, gastroenteropancreatic tumors and other tumors of neuroendocrine origin.^{3–6} The design of radiolabeled peptide constructs was based on peptide fragments of the natural ligands for the receptor, namely, cholecystokinin-8 (Asp-Tyr-Met-Gly-Trp-Met-Asp-Phe-NH₂, CCK-8) and human minigastrin (Leu-Glu-Glu-Glu-Glu-Ala-Tyr-Gly-Trp-Met-Asp-Phe-NH₂, MG). Both contain the C-terminal sequence Trp-Met-Asp-Phe-NH₂, which is necessary for receptor binding.^{7–9} To identify a peptide analogue combining high CCK2R affinity with an optimal pharmacokinetic profile, specific synthetic modifications have been introduced into the peptide sequences.^{10–12} These attempts mainly focused on MG, which has more favorable targeting properties compared to CCK8.^{13,14}

Already more than 2 decades ago, the high potential to target CCK2R with radiolabeled MG analogues was confirmed in clinical investigations.^{8,15} Early developed radiolabeled MG analogues based on [D-Glu¹]MG (MG0) showed a particularly high retention in the kidneys and therefore needed further refinement. The high renal uptake of these MG analogues could be associated with the N-terminal penta-Glu motif in positions 2–6 of the peptide.¹⁶ Removal of this part of the sequence efficiently reduced the kidney uptake and also led to a substantial reduction of the stability *in vivo* connected with a reduced tumor uptake.^{17,18} The simple inversion of the configuration of these five N-terminal amino acids from L-Glu to D-Glu led to the peptide derivatives [D-Glu^{1–6}]MG (CP04, formerly PP-F11) and [D-Glu^{1–6},Nle¹¹]MG (PP-F11N).^{19–21} In preclinical investigations, a strongly reduced renal retention and thus an improved biodistribution profile together with moderate stability against enzymatic degradation was reported

Received: July 15, 2020

Published: November 23, 2020



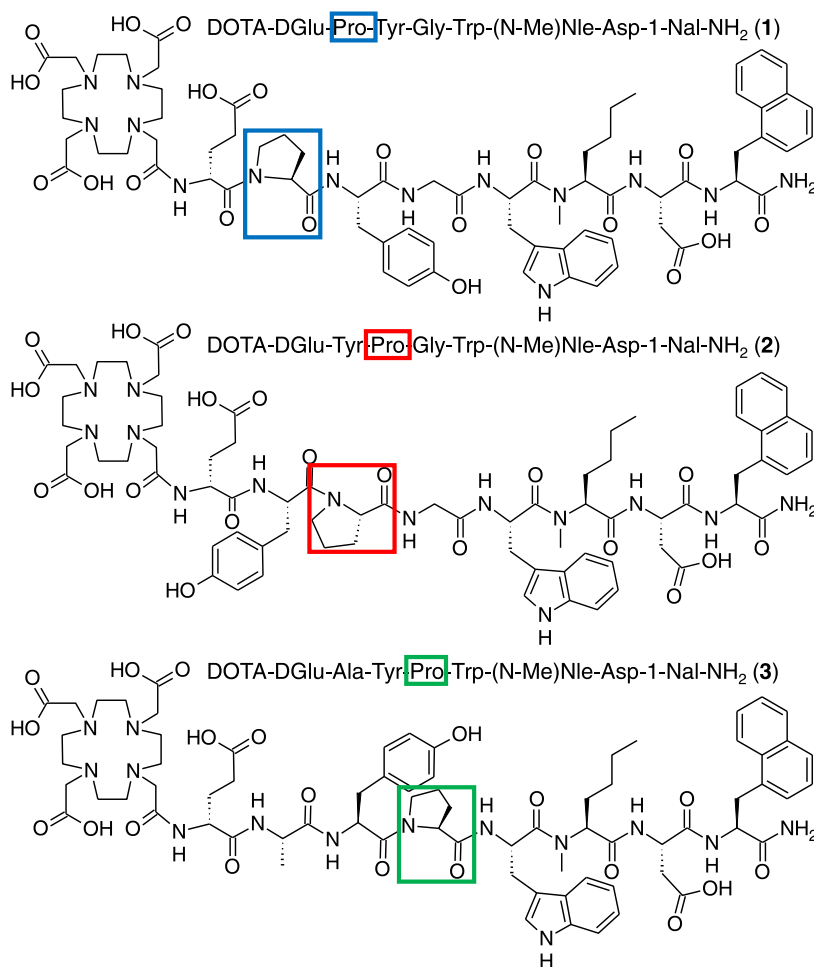


Figure 1. Structural formulas and amino acid sequences of 1–3.

for both peptide derivatives.^{11,20,22} Therefore, clinical studies with ¹¹¹In-labeled CP04 (ClinicalTrials.gov identifier: NCT03246659) and ¹⁷⁷Lu-labeled PP-F11N (ClinicalTrials.gov identifier: NCT02088645) have been initiated, investigating the safety as well as the diagnostic and therapeutic potential of these CCK2R-targeting radiopharmaceuticals.^{23,24}

A major issue only partly addressed in former optimization approaches is the limited enzymatic stability of MG within the C-terminal receptor-specific sequence potentially affecting the targeting properties.^{12,25} As previously reported by our group, it is possible to hinder the metabolization of this vulnerable part of the peptide by introducing bulky unnatural aromatic amino acids as well as N-methylated amino acids.^{26–28} Most interestingly, the introduction of such amino acids within the receptor-binding sequence resulted in novel MG analogues, which besides increased resistance against enzymatic degradation, also showed an enhanced receptor interaction, leading to increased cell uptake of the radiolabeled peptides in CCK2R-expressing cell lines. Comprehensive preclinical investigations evaluating the new modifications introduced within this part of the peptide sequence led to very promising results.^{26,27} Based on the truncated MG analogue [D¹Glu¹,DesGlu^{2–6}]MG (MG11), the peptide derivative MGS5 substituted with (N-Me)Nle in position 11 and 1-Nal in position 13 was developed. MGS5 conjugated to the bifunctional chelator 1,4,7,10-tetraazacyclododecane-1,4,7,10-tetraacetic acid (DOTA) radiolabeled with different radiometals showed a highly

improved biodistribution profile. The remarkable enhancement in CCK2R-related tumor uptake was combined with low unspecific tissue uptake, leading to very favorable tumor-to-background activity ratios. These improvements were independent of the radiometal-chelator approach used for radiolabeling.^{27,28} Introduction of an additional N-methylated peptide bond between Asp in position 12 and 1-Nal in position 13 further increased the resistance against enzymatic degradation *in vivo* and the tumor uptake. However, also the kidney uptake was drastically increased, a drawback especially with regard to therapeutic applications.²⁸

Since further modification within the C-terminal four amino acids of the peptide sequence may potentially affect the receptor affinity and additional introduction of N-methylated peptide bonds has shown to negatively impact pharmacokinetics, our current research activities focus on the introduction of alternative tertiary amide bonds in other parts of the peptide sequence.

Tertiary peptide bonds are formed naturally when the amino acid proline, containing a cyclic pyrrolidine side chain, is part of the peptide backbone. The presence of Pro leads to increased conformational rigidity,^{29,30} which—in analogy to small cyclic peptide analogues of somatostatin or MG^{31,32}—can be expected to enhance the stability toward enzymatic degradation. Within the peptide sequence of human MG, Ala in position 7, Tyr in position 8, and Gly in position 9, similarly to Pro, are uncharged amino acids. We have therefore

investigated the impact of additional introduction of Pro in these three different positions of the peptide. When substituting Tyr in position 8 with Pro, Tyr was shifted to position 7 in replacement of Ala to maintain the hydrophilicity of the peptide sequence. In this work, we present the outcome of the preclinical studies with three new peptide constructs derived from DOTA-MGSS by applying Pro substitution in different N-terminal positions. The effect of Pro substitution on the CCK2R affinity and cell uptake, as well as the biodistribution profile and tumor targeting of the radiolabeled peptide derivatives were investigated in tumor-xenografted mice. Major attention was directed toward the characterization of the enzymatic stability *in vivo*. Owing to the importance of stability mainly for the therapeutic application, the peptide derivatives conjugated to the bifunctional chelator DOTA and radiolabeled with indium-111 and lutetium-177 were characterized in this study.

RESULTS

Solid-Phase Peptide Synthesis (SPPS) and Radio-labeling. The chelator-conjugated peptide analogues were obtained in moderate yield (~15%) using Fmoc solid-phase peptide synthesis (SPPS). The molecular structure, amino acid sequence, and analytical data for the DOTA-peptides are presented in Figure 1 and Table 1. The amino acid sequence

Table 1. Summary of the Analytical Data of 1–3

| compound | purity (%) | calculated mass | found mass | HPLC t_R (min) |
|----------|------------|-----------------|-----------------------------|------------------|
| 1 | 96.6 | 1474.7 | 1476.9 [M + H] ⁺ | 16.9 |
| 2 | 98.2 | 1474.7 | 1476.9 [M + H] ⁺ | 16.9 |
| 3 | 95.3 | 1488.7 | 1490.9 [M + H] ⁺ | 16.8 |

was defined per synthesis protocol. High-performance liquid chromatography (HPLC) chromatograms and mass spectrometry (MS) spectra are presented in the Supporting Information (Figure S1).

Radiolabeling with lutetium-177 and indium-111 was carried out at 95 °C for 15–20 min with a radiochemical purity (RCP) of ≥95% and a nonoptimized molar activity of 11 GBq/μmol for ¹¹¹In-labeled and 55 GBq/μmol for ¹⁷⁷Lu-labeled compounds. For *in vivo* biodistribution studies, the radiolabeled peptides were purified by solid-phase extraction (SPE). Radiochromatograms are presented in the Supporting Information (Figure S2).

Characterization of the *In Vitro* Properties and Stability Studies in Different Media. First, *in vitro* investigations were performed with the ¹¹¹In-labeled peptide derivatives. A summary of the results is shown in Table 2. The stability analysis in phosphate-buffered saline (PBS) and

human serum showed high stability of the radiometal complex. Only minor enzymatic degradation with ≥97% intact radiopeptide occurred in serum after 24 h incubation for [¹¹¹In]In-1, [¹¹¹In]In-2 and [¹¹¹In]In-3. The radiopeptides showed a very similar hydrophilicity in relation to their distribution coefficient (log *D*) with values in the order of [¹¹¹In]In-3 (−2.05 ± 0.08) > [¹¹¹In]In-1 (−2.03 ± 0.10) > [¹¹¹In]In-2 (−1.75 ± 0.10), which corresponds to the minor differences in HPLC retention times (~17.1 min). The radiopeptides also showed very similar protein binding at the different time points investigated. After 24 h incubation, protein binding in the order of [¹¹¹In]In-3 (46.0 ± 0.5%) < [¹¹¹In]In-1 (52.8 ± 0.2%) < [¹¹¹In]In-2 (53.4 ± 0.2%) was found.

A higher degree of enzymatic degradation was observed for [¹¹¹In]In-1 and [¹⁷⁷Lu]Lu-1 as well as [¹¹¹In]In-2 and [¹⁷⁷Lu]Lu-2 in rat kidney and liver homogenates as analyzed for up to 120 min after incubation. The amount of intact radiopeptide found at each time point is presented in Figure 2. In rat liver homogenates, only minor differences between 1 and 2 were observed regardless of the radionuclide used for labeling with values of intact radiopeptide between 39 and 53% for 1 and 50 and 61% for 2 after 120 min incubation. A much faster degradation occurred in kidney homogenate, with values of ~5% intact radiopeptide for [¹¹¹In]In-1 and [¹⁷⁷Lu]Lu-1 and values between 25 and 34% for [¹¹¹In]In-2 and [¹⁷⁷Lu]Lu-2. In the radio-HPLC chromatograms, mainly one metabolite with a retention time of 15 min was formed for each radiopeptide (see Figure S3, Supporting Information). Despite the higher exposure to extracellular and intracellular proteases released after tissue homogenization, a similar trend of metabolization was found for ¹¹¹In- and ¹⁷⁷Lu-labeled 1 and 2. The obtained results justified further animal studies analyzing the stability of all three peptide derivatives *in vivo*.

Receptor Binding and Calcium Mobilization Assays.

Apparent half-maximal inhibitory concentration (IC₅₀) values evaluated in competition assays against [¹²⁵I][3-iodo-Tyr¹²,Leu¹⁵]gastrin-I on A431-CCK2R cells using unlabeled 1–3 are in the low-nanomolar range confirming a high affinity of these new CCK2R-targeting compounds. The mean IC₅₀ values obtained from three independent assays were 1.4 ± 0.6 nM for 1, 0.6 ± 0.3 nM for 2, and 1.3 ± 0.8 nM for 3. Representative binding curves are displayed in Figure 3. In previous assays with pentagastrin (1.0 ± 0.2 nM), DOTA-MG11 (0.9 ± 0.3 nM) and DOTA-MGSS (0.4 ± 0.2 nM), comparable values were found.²⁷

Calcium mobilization assays performed on A431-CCK2R stably transfected with human CCK2R and AR42J cells expressing rat CCK2R revealed that 1–3 provoked an intracellular Ca²⁺-mobilization already at a low peptide concentration (~1 nM) followed by a stable and lasting increase in Ca²⁺ concentration, leading to a plateau phase

Table 2. Summary of the Analytical Data of [¹¹¹In]In-1, [¹¹¹In]In-2 and [¹¹¹In]In-3 in Comparison with [¹¹¹In]In-DOTA-MGSS²⁷

| compound | log <i>D</i> | protein binding (%) | | intact radiopeptide in human serum (%) | | intact radiopeptide in PBS (%) | |
|----------------------------------|--------------|---------------------|------------|--|------|--------------------------------|------|
| | | 4 h | 24 h | time after incubation | | 24 h | 24 h |
| | | | | 4 h | 24 h | | |
| [¹¹¹ In]In-DOTA-MGSS | −2.03 ± 0.12 | 41.0 ± 0.2 | 44.3 ± 0.3 | 96.6 ± 0.8 | 95.5 | 96.6 ± 0.8 | 95.5 |
| [¹¹¹ In]In-1 | −2.03 ± 0.10 | 44.5 ± 1.8 | 52.8 ± 0.2 | 98.0 ± 0.3 | 98.0 | 98.1 ± 0.8 | 97.6 |
| [¹¹¹ In]In-2 | −1.75 ± 0.10 | 56.8 ± 0.1 | 53.4 ± 0.2 | 98.1 ± 0.8 | 97.6 | 96.5 ± 0.1 | 99.5 |
| [¹¹¹ In]In-3 | −2.05 ± 0.08 | 41.2 ± 0.1 | 46.0 ± 0.5 | 96.5 ± 0.1 | 99.5 | | |

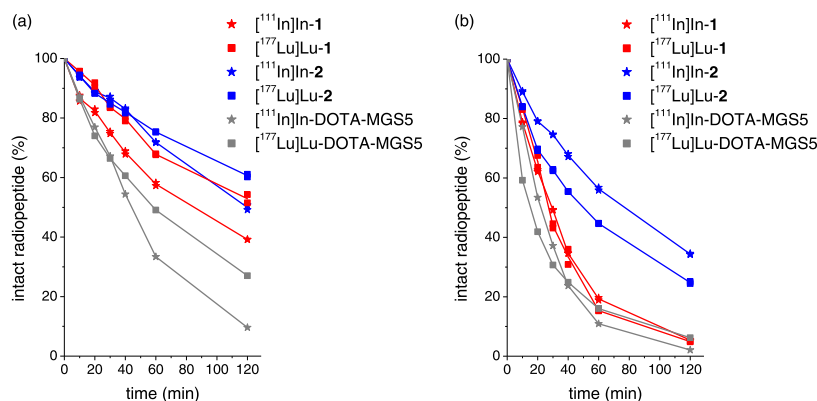


Figure 2. Intact radiopeptide after incubation at 37 °C in (a) rat liver homogenate and (b) rat kidney homogenate for $[^{111}\text{In}]\text{In-1}$ (red star), $[^{177}\text{Lu}]\text{Lu-1}$ (red square), $[^{111}\text{In}]\text{In-2}$ (blue star), and $[^{177}\text{Lu}]\text{Lu-2}$ (blue square); for comparison, previously reported data of $[^{111}\text{In}]\text{In-DOTA-MGS5}$ (gray star) and $[^{177}\text{Lu}]\text{Lu-DOTA-MGS5}$ (gray square) are added.²⁷

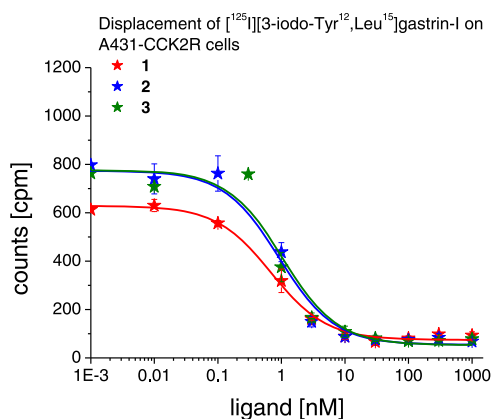


Figure 3. Representative binding curves obtained for 1 (red), 2 (blue), and 3 (green) on A431-CCK2R cells.

when increasing the peptide concentration. As shown in Table 3, EC_{50} values between 12.3 and 14.2 nM were obtained in the

Table 3. EC_{50} Values as Calculated from Dose-Related Calcium Mobilization Assays Performed on A431-CCK2R and AR42J Cells of 1–3 and Pentagastrin

| compound | EC_{50} (nM) | |
|---------------------------|-----------------------|-------------|
| | A431-CCK2R cells | AR42J cells |
| 1 ^a | 12.34 ± 2.40 | 1.74 ± 0.81 |
| 2 ^a | 14.23 ± 2.07 | 1.91 ± 0.49 |
| 3 ^b | 12.38 ± 3.83 | 1.27 ± 0.72 |
| pentagastrin ^c | 2.80 ± 0.52 | 0.43 ± 0.19 |

^a $n = 5$. ^b $n = 3$. ^c $n = 10$.

transfected A431-CCK2R cell line, whereas in rat AR42J cells, EC_{50} values between 1.3 and 1.9 nM were found. The difference in EC_{50} values between the two cell lines is in accordance with values found for the control pentagastrin (A431-CCK2R cells: 2.80 ± 0.52 nM; AR42J cells: 0.43 ± 0.19 nM) and can be explained by different post-translational modifications of the receptor protein in transfected cells and cells with physiological receptor expression.

In both cell lines, 1–3 exhibited an efficacy similar to that obtained with pentagastrin, suggesting an agonistic behavior for all three peptide analogues. Dose–response curves and

maximal Ca^{2+} response in relation to pentagastrin observed in both cell lines are displayed in Figure 4.

Cell Uptake Studies. In accordance with retained high CCK2R affinity, radiolabeled 1–3 showed a high and persistent uptake in the CCK2R transfected cell line A431-CCK2R. $[^{111}\text{In}]\text{In-1}$, $[^{111}\text{In}]\text{In-2}$, and $[^{111}\text{In}]\text{In-3}$ showed a cell internalization increasing over time with values of >10% after 15 min and up to ≥60% after 4 h of incubation. In mock-transfected A431 cells incubated under the same conditions and therefore serving as negative control, an uptake of <0.9% was observed for all radiopeptides at each time point, confirming a highly receptor-specific cell uptake. Representative internalization assays for the investigated radiopeptides are depicted in Figure 5.

Stability Studies in BALB/c Mice. In the *in vivo* stability studies performed with ^{111}In -labeled 1 and 2 at 10 min p.i., only minor differences in the resistance against enzymatic degradation were observed. A high amount of intact radiopeptide was found in blood ($[^{111}\text{In}]\text{In-1}$: 80.0 ± 5.2%; $[^{111}\text{In}]\text{In-2}$: 82.3 ± 1.8%) and liver ($[^{111}\text{In}]\text{In-1}$: 76.0 ± 0.4%; $[^{111}\text{In}]\text{In-2}$: 73.9 ± 1.2%), whereas a faster degradation was observed in kidneys ($[^{111}\text{In}]\text{In-1}$: 23.4 ± 4.2%; $[^{111}\text{In}]\text{In-2}$: 30.2 ± 0.5%) and urine ($[^{111}\text{In}]\text{In-1}$: 21.8 ± 8.1%; $[^{111}\text{In}]\text{In-2}$: 30.3 ± 5.9%). As described for rat organ homogenates, a major metabolite with a retention time of 15 min was confirmed in kidneys and liver. The *in vivo* studies allowed us to monitor some additional metabolites with lower retention time around 5 min. Radiochromatograms showing the amount of intact $[^{111}\text{In}]\text{In-1}$ and $[^{111}\text{In}]\text{In-2}$ in blood, liver, kidneys, and urine of female BALB/c mice at 10 min p.i. are displayed in the Supporting Information (Figure S4).

Further studies were carried out to investigate the enzymatic stability of the ^{177}Lu -labeled peptide analogues also for later time points after injection. These studies were carried out for all three ^{177}Lu -labeled peptide derivatives for the time points of 30 and 60 min after injection. The highest amount of intact radiopeptide was found for $[^{177}\text{Lu}]\text{Lu-2}$ with values of 79.1% in blood, 74.5% in liver, 11.0% in kidneys, and 18.8% in urine after 60 min incubation. At the same time point, the amounts of intact radiopeptide for $[^{177}\text{Lu}]\text{Lu-1}$ and $[^{177}\text{Lu}]\text{Lu-3}$ were 56.6 and 63.5% in blood, 30.8 and 35.6% in liver, 8.1 and 7.2% in the kidneys, and 23.0 and 20.6% in urine. The radiochromatograms showing the amount of intact radiopeptide found for $[^{177}\text{Lu}]\text{Lu-1}$, $[^{177}\text{Lu}]\text{Lu-2}$, and $[^{177}\text{Lu}]\text{Lu-3}$ in blood,

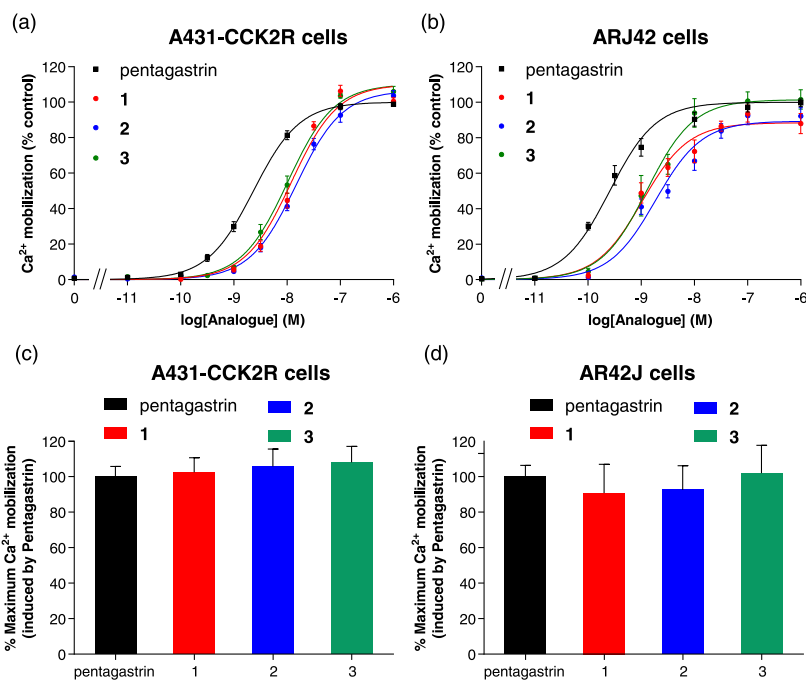


Figure 4. Calcium mobilization assays: dose–response curves obtained with (a) A431-CCK2R cells and (b) AR42J cells, as well as maximal Ca^{2+} response in relation to pentagastrin for (c) A431-CCK2R cells and (d) AR42J cells; pentagastrin (black), 1 (red), 2 (blue), and 3 (green).

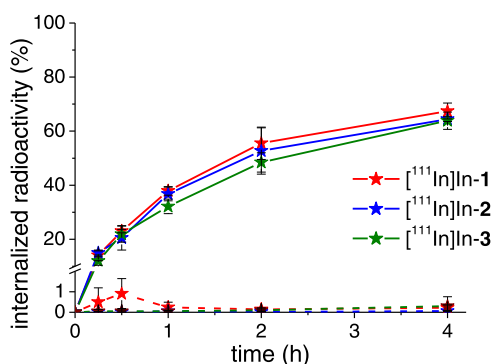


Figure 5. Cell uptake over time of ^{111}In -labeled 1 (red), ^{111}In -labeled 2 (blue), and ^{111}In -labeled 3 (green) in A431-CCK2R cells (solid line) and A431-mock cells (dashed line) expressed as % of the total activity added ($n = 3$).

liver, kidneys, and urine of female BALB/c mice at 60 min p.i. are presented in Figure 6.

A prolonged stabilization against enzymatic degradation *in vivo* could be confirmed for all three radiopeptides. The studies were only conducted with one mouse for each time point and therefore do not allow conclusions to be drawn about differences between the three radiopeptides. A summary showing the amount of intact ^{177}Lu -labeled 1, ^{177}Lu -labeled 2, and ^{177}Lu -labeled 3 for both time points of 30 min and 60 min p.i. can be found in the Supporting Information (Figure S5).

Biodistribution in BALB/c Nude Mice Bearing A431-CCK2R/Mock Xenografts. Biodistribution studies in A431-CCK2R/A431-mock-xenografted female BALB/c nude mice with an injected peptide amount of 20 pmol for the time point of 4 h p.i. were conducted for ^{177}Lu -labeled 1–3 as well as ^{111}In -labeled 1 and 2. For ^{177}Lu -labeled 1 and ^{177}Lu -labeled 2, additional studies at the later time point of 12 h p.i. as well as at a higher peptide amount of 150 pmol were carried out. The tumor uptake and tissue distribution, as well as the tumor-to-

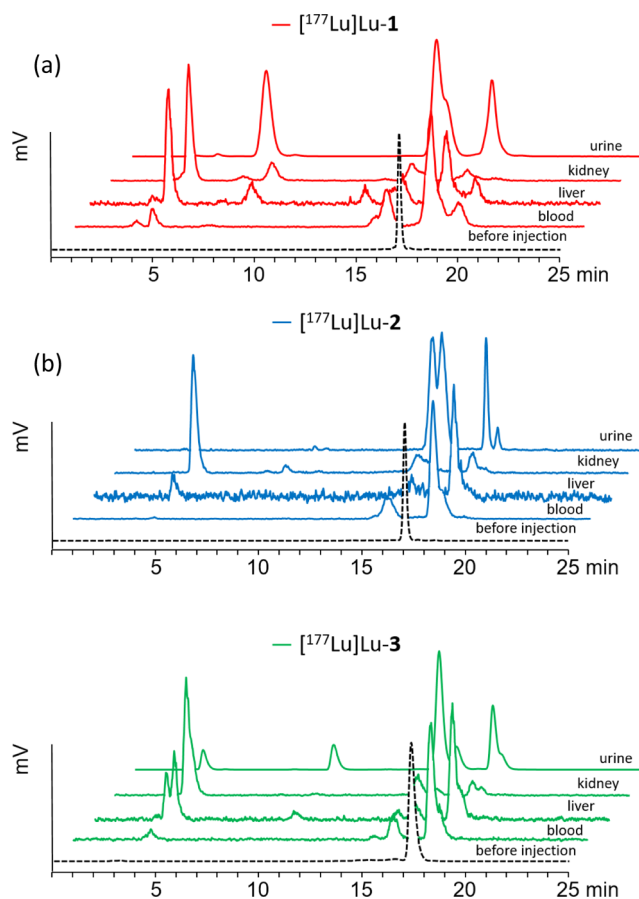


Figure 6. Results of *in vivo* stability studies in BALB/c mice showing the intact radiopeptide in blood, liver, kidney, and urine at 60 min p.i. for (a) ^{177}Lu -labeled 1 (red), (b) ^{177}Lu -labeled 2 (blue), and (c) ^{177}Lu -labeled 3 (green).

Table 4. Results of Biodistribution Studies Evaluated in A431-CCK2R/A431-Mock Xenografted BALB/c Nude Mice of the ^{177}Lu - and ^{111}In -Labeled Peptide Derivatives (20 pmol, 4 h p.i.)^a

| compound | ^{177}Lu]Lu-1 | ^{177}Lu]Lu-2 | ^{177}Lu]Lu-3 | ^{111}In]In-1 | ^{111}In]In-2 |
|------------------|-------------------------|-------------------------|-------------------------|-------------------------|-------------------------|
| blood | 0.07 ± 0.02 | 0.08 ± 0.01 | 0.06 ± 0.03 | 0.07 ± 0.02 | 0.07 ± 0.02 |
| lung | 0.14 ± 0.05 | 0.17 ± 0.01 | 0.17 ± 0.05 | 0.18 ± 0.02 | 0.20 ± 0.02 |
| heart | 0.09 ± 0.01 | 0.09 ± 0.01 | 0.08 ± 0.01 | 0.08 ± 0.01 | 0.09 ± 0.01 |
| muscle | 0.06 ± 0.05 | 0.06 ± 0.03 | 0.09 ± 0.05 | 0.07 ± 0.03 | 0.04 ± 0.02 |
| spleen | 0.18 ± 0.04 | 0.16 ± 0.01 | 0.19 ± 0.02 | 0.18 ± 0.00 | 0.18 ± 0.05 |
| intestine | 1.14 ± 0.51 | 0.56 ± 0.10 | 0.95 ± 0.23 | 0.81 ± 0.60 | 0.56 ± 0.06 |
| liver | 0.42 ± 0.06 | 0.43 ± 0.08 | 0.52 ± 0.12 | 0.39 ± 0.07 | 0.41 ± 0.06 |
| kidney | 3.97 ± 1.31 | 5.53 ± 1.51 | 6.61 ± 1.75 | 3.74 ± 0.44 | 5.00 ± 0.41 |
| pancreas | 2.09 ± 0.84 | 1.21 ± 0.49 | 1.78 ± 0.72 | 2.14 ± 2.20 | 1.18 ± 0.22 |
| stomach | 7.37 ± 2.26 | 4.68 ± 0.93 | 4.73 ± 2.29 | 9.07 ± 2.60 | 8.40 ± 0.52 |
| A431-CCK2R | 34.72 ± 9.40 | 33.25 ± 6.34 | 28.60 ± 7.95 | 42.81 ± 9.25 | 46.29 ± 8.16 |
| A431-mock | 0.32 ± 0.14 | 0.25 ± 0.06 | 0.25 ± 0.06 | 0.36 ± 0.12 | 0.29 ± 0.03 |
| tumor-to-blood | 540 ± 103 | 429 ± 134 | 709 ± 470 | 640 ± 222 | 690 ± 270 |
| tumor-to-liver | 83.3 ± 23.0 | 80.6 ± 26.5 | 58 ± 19.2 | 109 ± 16 | 115 ± 31 |
| tumor-to-kidney | 9.58 ± 3.84 | 6.51 ± 2.29 | 4.52 ± 1.41 | 11.6 ± 3.0 | 9.33 ± 1.98 |
| tumor-to-stomach | 5.22 ± 2.68 | 7.31 ± 1.84 | 6.49 ± 1.32 | 5.02 ± 1.90 | 5.49 ± 0.71 |

^aValues are expressed as % IA/g (mean ± standard deviation (SD), $n = 4$).

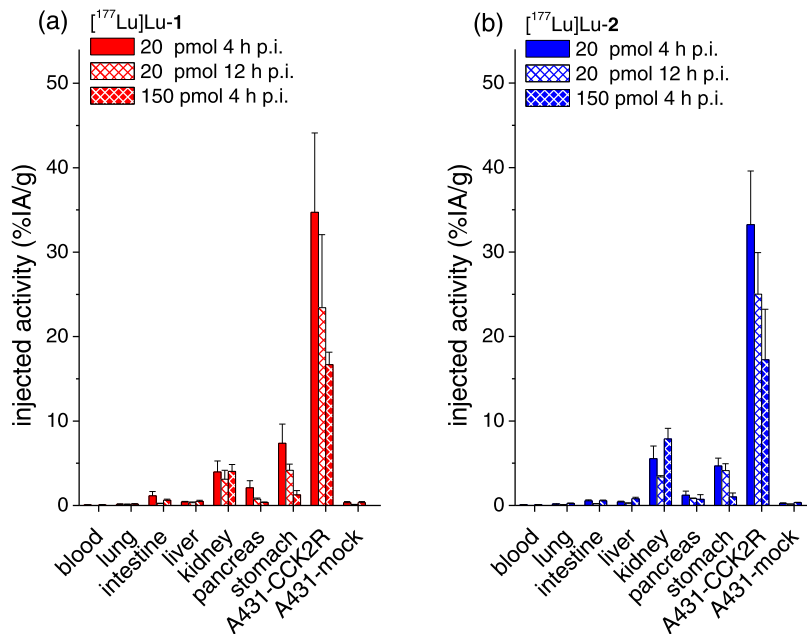


Figure 7. Tumor uptake and tissue distribution in selected organs obtained from biodistribution studies in A431-CCK2R/A431-mock xenografted BALB/c nude mice for (a) ^{177}Lu]Lu-1 and (b) ^{177}Lu]Lu-2, at different time points and injected peptide amounts. Values are expressed as % IA/g (mean ± SD, $n = 4$).

organ ratios are summarized in Table 4 and Figure 7. Additional data can be found in the Supporting Information (Table S1). All three radiopeptides were rapidly excreted from the body, mainly through the kidneys, resulting in low uptake in most organs. The uptake values found for A431-CCK2R xenografts (tumor weight: 0.24 ± 0.16 g) were in the order of ^{177}Lu]Lu-1 ($34.72 \pm 9.40\%$ IA/g) > ^{177}Lu]Lu-2 ($33.25 \pm 6.34\%$ IA/g) > ^{177}Lu]Lu-3: ($28.60 \pm 7.95\%$ IA/g). These differences were however not statistically significant ($p > 0.8$). A very low unspecific uptake <0.5% IA/g was observed in A431-mock xenografts (tumor weight: 0.33 ± 0.24 g). The CCK2R-specific uptake of the three radiopeptides in stomach (5–7% IA/g) and pancreas (1–2% IA/g) was comparable. Additionally, a moderate uptake occurred in kidneys (4–7% IA/g).

Based on the more favorable tumor-to-kidney ratios found for ^{177}Lu]Lu-1 and ^{177}Lu]Lu-2, these two peptide derivatives were selected for additional studies with indium-111, as well as studies at a later time point after injection and at a higher injected peptide amount when labeled with lutetium-177.

Also under these conditions, a rapid renal excretion with fast washout from most tissues occurred. ^{111}In]In-1 ($42.81 \pm 9.25\%$ IA/g) and ^{111}In]In-2 ($46.29 \pm 8.16\%$ IA/g) displayed a somewhat higher uptake in A431-CCK2R xenografts (tumor weight: 0.15 ± 0.03), which was statistically significant only for ^{111}In]In-2 ($p = 0.045$). ^{111}In]In-1 showed a significantly reduced kidney uptake compared to ^{111}In]In-2 ($p = 0.006$).

^{177}Lu]Lu-1 and ^{177}Lu]Lu-2, analyzed at a later time point of 12 h p.i., revealed a good washout of the radioactivity over time, as shown by the significant reduction of the radioactivity

in blood ($p < 0.003$) observed for both radiopeptides. A good tumor retention of $>60\%$ was observed for both [^{177}Lu]Lu-1 ($23.43 \pm 8.64\%$ IA/g) and [^{177}Lu]Lu-2 ($25.02 \pm 4.92\%$ IA/g). A significant reduction of the organ uptake was further found in stomach for [^{177}Lu]Lu-1 ($p = 0.036$) and in kidneys for [^{177}Lu]Lu-2 ($p = 0.030$).

When increasing the injected peptide amount to 150 pmol, some saturation effects occurred in CCK2R-expressing tissues. The tumor uptake in A431-CCK2R xenografts was reduced by about 50%, with values of $16.68 \pm 1.48\%$ IA/g ($p = 0.009$) for [^{177}Lu]Lu-1 and $15.26 \pm 6.84\%$ IA/g ($p = 0.010$) for [^{177}Lu]Lu-2, whereas no effect was observed in A431-mock xenografts. The saturation effects were even more prominent in CCK2R-expressing stomach and pancreas. Kidney uptake remained stable in the case of [^{177}Lu]Lu-1, but was significantly increased in the case of [^{177}Lu]Lu-2 ($p = 0.055$). [^{177}Lu]Lu-2 showed a significantly increased unspecific uptake also in spleen ($p = 0.029$) and liver ($p = 0.014$).

When comparing [^{177}Lu]Lu-1 and [^{177}Lu]Lu-2, at the different time points and injected peptide amounts studied, kidney uptake and tumor-to-kidney ratio were in favor for [^{177}Lu]Lu-1, whereas no relevant differences were observed for the tumor-to-stomach ratio of both radiopeptides.

DISCUSSION

A common strategy in the development of radiotracers suitable for nuclear medical applications is to use natural ligands with high affinity for a selected target as molecular templates, which are then chemically modified.^{33,34} Modifications are necessary to meet basic requirements such as stable labeling with radionuclides as well as high resistance of the molecular structure against enzymatic degradation. Conjugation to bifunctional chelators allows for fast labeling in high yields with corresponding radiometals, applicable for single photon emission computed tomography (SPECT), positron emission tomography (PET), and targeted radiotherapy and is therefore frequently used for peptide-based radiotracers.^{35,36} To achieve the required *in vivo* stability and bioavailability, a variety of different strategies such as the introduction of unnatural amino acids or amino acids in D-configuration, shortening of the peptide sequence or the introduction of linkers, cyclization, as well as the inclusion of modified peptide bonds such as 1,2,3-triazoles or N-methylated bonds have been explored.

Especially for CCK2R-targeting peptide analogues, different strategies have been investigated over the last 2 decades to further optimize the biodistribution profile and targeting properties of the ligands for theranostic applications in patients with MTC and other CCK2R-related malignancies.^{1,20,27,36–39}

In recent studies performed by our group, it has been demonstrated that it is possible to strongly increase the enzymatic stability of MG analogues by introducing N-methylated tertiary peptide bonds in the C-terminal receptor-specific sequence, which leads to a significantly increased tumor uptake as shown for DOTA-MGS4, DOTA-MGSS, or HYNIC-MGS11.^{26–28} Recently, the introduction of modified peptide bonds within the structure of MG was also studied by another group. Insertion of 1,2,3-triazoles in different positions of the peptide backbone resulted in MG analogues showing advantageous properties in preclinical studies.^{39,40} Within this study, we have extended the approach of introducing stabilizing tertiary peptide bonds to the insertion of proline, the only proteinogenic amino acid that naturally forms tertiary peptide bonds. In the new peptide

analogues, the C-terminal substitutions of DOTA-MGSS, which are associated with strongly increased bioavailability as well as a favorable biodistribution profile,²⁷ were combined with further Pro substitutions in the N-terminal part of the peptide sequence. The receptor affinity studies confirmed that Pro substitution in different N-terminal positions does not affect CCK2R affinity. Similar results were also obtained in previous studies investigating the receptor affinity of CCK2R-targeting peptide derivatives with different modifications, such as changes of the N-terminal amino acids, dimerization, or cyclization of the peptide sequence, as long as only minor changes were applied in the C-terminal region Trp-Met-Asp-Phe-NH₂. The receptor affinity of all three peptide analogues with IC₅₀ values of ~ 1 nM well compared to pentagastrin, DOTA-MG11 and DOTA-MGSS. In calcium mobilization assays, an agonistic behavior was confirmed for all three compounds. The lower potency of the new derivatives tested in cell lines expressing rat or human CCK2R compared to pentagastrin is possibly related to the changes applied in the C-terminal region.

DOTA-MGSS shows reduced hydrophilicity compared to other MG analogues like DOTA-MG11 ($\log D = -2.03 \pm 0.12$ vs -3.55 ± 0.23 of the corresponding ^{111}In -labeled compounds^{26,27}). To avoid a further reduction in hydrophilicity of the new MG derivatives, only nonpolar amino acids, such as Ala in position 7 and Gly in position 9, were selected for further substitution by Pro. These amino acids form highly flexible peptide bonds due to their small aliphatic side chains. Substitution with Pro leads to increased rigidity of the peptide chain; thus, increased stability could be expected. Furthermore, we aimed to investigate substitution with Pro also for position 8. To maintain hydrophilicity, Tyr was shifted to position 7 replacing Ala, thus allowing us to introduce Pro in position 8. The corresponding CCK2R ligand can be classified as a CCK8 derivative. The results of the *in vitro* characterization confirmed a hydrophilicity comparable to DOTA-MGSS, with a $\log D$ value ~ 2 for all three ^{111}In -labeled compounds. High stability of the metal complex was observed for incubation in PBS together with a similar binding to serum proteins of all three compounds with values of $\sim 50\%$, comparable to [^{111}In]In-DOTA-MGSS. The new derivatives also showed high stability when incubated in human serum, with more than 95% intact radiopeptide still present after 24 h incubation.

When incubated in rat organ homogenates, a measure suitable to get a deeper insight into the resistance against enzymatic degradation, increased stability compared to ^{111}In -labeled as well as ^{177}Lu -labeled DOTA-MGSS, was observed for both 1 and 2 when labeled with the same radionuclides. These results indicate that additional insertion of tertiary peptide bonds is associated with increased stability against enzymatic degradation and justified further metabolic studies *in vivo*. During incubation in organ homogenates, the radiopeptides are exposed to a higher number of proteases, therefore extending the *in vitro* characterization of metabolic degradation. However, also intracellular proteases are considered, which might not affect the enzymatic degradation *in vivo*,^{2,41} potentially leading to an underestimation of the stability *in vivo*. Only limited information is available in the literature regarding the stability against enzymatic degradation of CCK2R-targeting peptides *in vivo*. Most of the *in vivo* studies with other radiopeptides previously studied have been performed only for short time points after injection, such as 5–

10 min after injection. In this study, the metabolic stability *in vivo* was analyzed also for later time points of 30 and 60 min. Therefore, we can relate the results only to data generated by our group for DOTA-MGSS and CP04.²⁷ For all three Pro-substituted peptide analogues, comparable to DOTA-MGSS, a higher stability during circulation *in vivo* was observed, whereas a much higher degree of metabolization occurs during renal excretion. The comparison with [¹⁷⁷Lu]Lu-CP04, showing 5% intact radiopeptide in the blood of mice at 30 min p.i., best demonstrates the prominent increase in enzymatic stability.²⁷ The percentage of intact radiopeptide in blood of the new derivatives compares well with [¹⁷⁷Lu]Lu-DOTA-MGSS.²⁷ Some additional metabolites with higher retention time could be detected for the new peptide analogues, indicating an additional stabilization in the N-terminal area achieved by the insertion of Pro. In ongoing experiments, we are further characterizing the formed metabolites, as they may give hints for other alternative stabilizing modifications.

The influence of the new substitutions on the biodistribution profile was evaluated in BALB/c nude mice xenografted with A431-CCK2R and A431-mock cells. At the moment, this transfected cell line seems most suitable to evaluate the targeting potential, since no natural cell line expressing human CCK2R is currently available. This mouse-xenograft-model also includes a mock-transfected negative control, allowing us to demonstrate the specificity of tumor binding and has already been used for the evaluation of a variety of CCK2R-targeting peptide analogues allowing for comparison with data generated by other groups. When comparing the influence of Pro substitution in the different N-terminal positions with data obtained for DOTA-MGSS, a similar biodistribution profile in terms of nonspecific organ uptake as well as uptake in kidneys and CCK2R-expressing organs, stomach and pancreas, was found. However, the uptake in CCK2R-expressing tumor xenografts of the new radiolabeled peptide analogues with values ranging from 29 to 46% ID/g was increased by a factor of 1.2–1.9, possibly reflecting the improved stabilization against enzymatic degradation *in vivo*.²⁷ Compared to the tumor uptake in A431-CCK2R xenografts of 7–9% IA/g combined with a tumor-to-kidney ratio of 1–2 and a tumor-to-stomach ratio of 3–4 observed for [¹¹¹In]In-PP-F11 and [¹⁷⁷Lu]Lu-PP-F11N, two MG analogues currently investigated in clinical trials,^{20,22} the new MG analogues besides a clear increase in tumor uptake by a factor of 4–5 also show improved tumor-to-kidney (5–12) and tumor-to-stomach ratios (5–7). [¹⁷⁷Lu]Lu-3 showed the lowest tumor-to-kidney and tumor-to-liver ratio of the three tested peptide analogues and was therefore not further characterized in additional biodistribution studies at a later time point and at a higher injected peptide amount. When considering all three tested peptide analogues, [¹⁷⁷Lu]Lu-1 with a tumor uptake of 35% IA/g at 4 p.i. in combination with a tumor-to-kidney ratio of 10 and a tumor-to-stomach ratio of 5, seems to be most suitable for peptide receptor radionuclide therapy. The tumor retention at a later time point is in line with other CCK2R-targeting peptide analogues. For different ¹⁷⁷Lu-labeled and ¹¹¹In-labeled MG analogues, a comparable reduction of the radioactivity within the first 24 h after injection was reported for different tumor xenografts.^{37,42} The same applies for the saturation effects observed in A431-CCK2R xenografts and in stomach when injecting a higher peptide dose. Receptor-saturation with increasing injected peptide amounts has been reported also for other ¹¹¹In-labeled MG analogues, showing a

similar reduction of the tumor uptake in AR42J^{42,43} and A431-CCK2R xenografts.^{26,27,44}

CONCLUSIONS

In recent years, several successes have been achieved in the clinical translation of CCK2R ligands. Low enzymatic stability of the radioligands remains a major hurdle, and no therapeutic application has yet found its way into nuclear medicine routine. In this study, we could successfully show that the combination of the C-terminal modifications of DOTA-MGSS with additional N-terminal Pro substitution in different positions results in an improved biodistribution profile in the preclinical animal model. [¹⁷⁷Lu]Lu-1, displaying the highest tumor uptake and most favorable tumor-to-kidney ratio of the three different conjugates tested, seems most promising for clinical translation. In parallel, in ongoing studies, we are characterizing the radiometabolites formed *in vivo* to better understand the underlying degradation mechanisms and possibly derive other alternative stabilization strategies.

EXPERIMENTAL SECTION

Materials and General Methods. All commercially obtained chemicals were of analytical grade and used without further purification unless otherwise stated. [¹¹¹In]InCl₃ was purchased from Mallinckrodt Medical (Petten, The Netherlands). No-carrier-added [¹⁷⁷Lu]LuCl₃ produced from highly enriched ytterbium-176 was provided by Isotope Technologies Garching (Munich, Germany). All synthesized compounds were characterized by matrix-assisted laser desorption/ionization time-of-flight mass spectrometry (MALDI-TOF-MS) and analytical HPLC and were obtained in a purity >95%.

For preparative HPLC purification, a Gilson 322 chromatography system (Gilson International, Limburg, Germany) with Gilson UV/vis-155 multiwavelength detector, equipped with an Eurosil Bioselect Vertex Plus C18A precolumn (300 Å, 5 μm, 30 × 8 mm²) and a Eurosil Bioselect Vertex Plus C18A column (300 Å, 5 μm, 300 × 8 mm²) (Knauer, Berlin, Germany) was used with a gradient system starting from 80% solvent A (water containing 0.1% trifluoroacetic acid (TFA)) and increasing concentrations of solvent B (acetonitrile (ACN) containing 0.1% TFA) with a flow rate 2 mL/min: 0–4 min 20% B, 4–24 min 20–60% B, 24–26 min 60% B, 26–27 min 60–80% B, 27–28 min 80% B, 28–29 min 80–20% B, 29–37 min 20% B.

Analytical HPLC was performed using an UltiMate 3000 chromatography system (Dionex, Germering, Germany) consisting of an HPLC pump, a variable UV detector (UV-vis at λ = 280 nm), an autosampler, and a radiodetector (GabiStar, Raytest, Straubenhardt, Germany), equipped with a Phenomenex Jupiter 4 μm Proteo C12 90 Å, 250 × 4.6 mm² column (Phenomenex Ltd., Aschaffenburg, Germany) using a flow rate of 1 mL/min together with the following gradient system: 0–3 min 10% B, 3–18 min 10–55% B, 18–20 min 80% B, 20–21 min 80–10% B, 21–25 min 10% B. The radiodetector was equipped with two different loops, a low-sensitivity loop of 5 μL and a high-sensitivity loop of 250 μL allowing for a better signal during analysis of samples with low activity obtained from stability studies *in vivo*.

For matrix-assisted laser desorption/ionization time-of-flight mass spectrometry (MALDI-TOF-MS) a Bruker microflex benchtop MALDI-TOF MS (Bruker Daltonics, Bremen, Germany) was used in reflector acquisition mode with a positive-ion source and 200 shots per spot. MALDI samples were prepared on an α-cyano-4-hydroxycinnamic acid (HCCA) matrix using the dried droplet procedure. Flex Analysis 2.4 software was used to analyze the recorded data.

Solid-Phase Peptide Synthesis. Compounds 1–3 were synthesized following a standard 9-fluorenylmethoxycarbonyl (Fmoc) solid-phase peptide synthesis (SPPS) protocol on Rink amide MBHA resin (Novabiochem, Hohenbrunn, Germany). The following protection groups for reactive side chains of selected amino

acids were used: *tert*-butyl ester for Asp and D₂Glu, *tert*-butyl ether for Tyr, and *tert*-butyloxycarbonyl (BOC) for Trp. Starting from 100 mg of resin (with capacity 0.65 mmol/g), all coupling reactions were performed using a 5-fold excess of Fmoc-protected amino acids, 1-hydroxy-7-aza-benzotriazole (HOAt) and *O*-(7-azabenzotriazole-1-yl)-*N,N,N',N'*-tetramethyluronium hexa-fluorophosphate (HATU) in *N*-methyl-2-pyrrolidone (NMP) pH adjusted to 8–9 with *N,N'*-diisopropylethylamine. Fmoc-protected amino acids following (*N*-Me)Nle were coupled twice. For the coupling of DOTA, a 3-fold molar excess of DOTA-tris(*t*-Bu)ester, HOAt and HATU, was used. Cleavage of the peptide conjugates from the resin and removal of acid-labile protecting groups was performed with a mixture consisting of TFA, triisopropylsilane, and water in a ratio of 95/2.5/2.5 v/v/v. The crude products were precipitated and washed with ice-cold diethyl ether, followed by preparative and analytical HPLC to purify and characterize the synthesized peptide conjugates. The identity of the final product was confirmed by MALDI-TOF MS and, the product was lyophilized and stored at –20 °C in a fraction of 0.5–1 mg.

Radiolabeling. For labeling with indium-111 and lutetium-177, 1–3 (10–20 µg) were incubated with ≤120 µL of the corresponding radiometal in hydrochloric acid solution (30–70 MBq [¹¹¹In]InCl₃, 0.05 M HCl; 100–350 MBq [¹⁷⁷Lu]LuCl₃, 0.04–0.05 M HCl). A 1.2-fold volume of a 0.4 M sodium acetate/0.24 M gentisic acid solution adjusted to pH 5 was added (total volume <0.3 mL), and the mixture was heated at 95 °C for 20 min. Radiochemical analysis of the radiolabeled peptide conjugates was performed using the analytical HPLC system. For biodistribution studies, an SPE purification of the radiolabeled peptides was performed to remove any free radiometal. Therefore, the radiolabeling mixture was diluted to 1 mL with saline and passed through a C18 SepPak Light cartridge (Waters, Milford), pretreated with 5 mL of ethanol and 5 mL of saline. The cartridge was washed with 2 mL of saline, the radiolabeled peptide eluted with 0.2–0.4 mL of 60–80% ethanol/phosphate-buffered saline (PBS) and diluted with saline or PBS to a final volume of 1–2 mL. This method efficiently removed all hydrophilic and non-peptide-related impurities. The solutions injected in mice further contained 0.1 mM sodium bicarbonate solution and a 20-fold excess of diethylenetriaminepentaacetic acid (DTPA).

Radiiodination of human [Leu¹⁵]gastrin-I (Bachem, Bubendorf, Switzerland) was carried out using the chloramine-T method and carrier-free Na[¹²⁵I]I (PerkinElmer, Boston, MA). After HPLC purification, [¹²⁵I][3-iodo-Tyr¹²,Leu¹⁵]gastrin-I at high molar activity was obtained and stored in aliquots at –20 °C (further details are presented in Figure S6, Supporting Information).

Cell Culture. The stably transfected A431 human epidermoid carcinoma cell line containing the plasmid pCR3.1 incorporating the full coding sequence for the human CCK2R (A431-CCK2R) and the same cell line transfected with the empty vector alone (A431-mock) kindly provided by Dr. Luigi Aloj were used as a cell model. A number of 4.7×10^6 binding sites per cell have been determined for A431-CCK2R cells in binding affinity studies.⁴⁵ The cell lines were cultured in 10% (v/v) fetal bovine serum and 5 mL of 100× penicillin–streptomycin–glutamine supplemented Dulbecco's modified Eagle's medium (DMEM) at 37 °C in a humidified 95% air/5% CO₂ atmosphere. AR42J rat pancreatic tumor cells (ECACC, Salisbury, U.K.), physiologically expressing the rat CCK2R were cultured in Roswell Park Memorial Institute (RPMI) 1640 medium containing the same supplements as described above at 37 °C in a humidified 95% air/5% CO₂ atmosphere. Subculturing of the cells was performed three times a week when cells approached confluence in a ratio of 1:2–1:3 using a 10× trypsin (2.5%) solution. Media and supplements were purchased from Fisher Scientific (Vienna, Austria).

Characterization of the *In Vitro* Properties and Stability Studies in Different Media. First, *in vitro* characterizations of 1–3 were performed after ¹¹¹In-labeling to generate data comparable to previously investigated MG analogues presented by our group. *In vitro* stability studies characterizing the complex stability as well as the metabolic stability of the radiolabeled peptide analogues were carried out in PBS, fresh human serum, and rat liver and rat kidney

homogenates. Organ homogenates were prepared from freshly dissected organs homogenized (IKA-Werke, Staufen, Germany) for 1 min at room temperature (RT) in a 20 mM 4-(2-hydroxyethyl)-1-piperazineethanesulfonic acid (HEPES) buffer at pH 7.3 (30% w/v). A fraction of 0.1 mL of radiolabeled peptide diluted in PBS/HEPES was added to 0.9 mL of medium reaching a final concentration of ~500 pmol/mL and incubated at 37 °C for up to 120 min in rat organ homogenates (*n* = 2) and up to 24 h in human serum or PBS (*n* = 1). At each time point, 100 µL of sample was taken treated with 150 µL of ACN to precipitate proteins centrifuged (2000g, 2 min), diluted with water (1:1), and a fraction of 100 µL was injected to the analytical HPLC system. For serum and tissue homogenates, only the soluble phase extracted after centrifugation was analyzed, whereas the radioactivity lost in the pellet was not considered.

To determine the log *D* of the ¹¹¹In-labeled peptide analogues, 500 µL of the radiolabeled peptide solution (50 pmol/mL in PBS) was added to 500 µL of octanol (1:1) and vigorously vortexed for 15 min (*n* = 8). After a time of 10 min sufficient for the separation of the two phases, 100 µL aliquots of both layers were measured in a γ counter (2480 Wizard² 3 in., PerkinElmer Life Sciences and Analytical Sciences, formerly Wallac Oy, Turku, Finland) and the distribution coefficient (log *D*) was calculated. The protein binding in human serum (500 pmol/mL, *n* = 2) was assessed by Sephadex G-50 size-exclusion chromatography (GE Healthcare Illustra, Little Chalfont, U.K.) for up to 24 h.

Receptor Binding and Calcium Mobilization Assays. The binding affinity of 1–3 was tested in competitive binding assays against [¹²⁵I][3-iodo-Tyr¹²,Leu¹⁵]gastrin-I on A431-CCK2R cells. Binding assays were carried in 96-well filter plates (Multi-ScreenHTS-FB, Merck Group, Darmstadt, Germany) pretreated with 10 mM TRIS/139 mM NaCl buffer, pH 7.4 (TRIS-buffer) (2 × 250 µL) before 400 000 A431-CCK2R cells per well were added in 35 mM HEPES buffer, pH 7.4, containing 10 mM MgCl₂, 14 µM bacitracin, and 0.5% bovine serum albumin (BSA).⁴⁶ Competition assays were performed three times in triplicate using increasing concentrations of competitor (0.003–1000 nM) and a constant amount of radioligand (~40 000 cpm). After 1 h of incubation at room temperature (RT), the medium was removed and the filters were rapidly rinsed with ice-cold TRIS-buffer (2 × 200 µL), removed and counted in a γ-counter. Half-maximal inhibitory concentration (IC₅₀) values were calculated following nonlinear regression with Origin software (MicroCal Origin 6.1, Northampton, MA). Even though incubation was performed in a hypoosmotic solution disturbing the integrity of the cell membrane, we cannot totally exclude that a limited extent of internalization affecting the binding equilibrium occurred. Therefore, the binding affinity measurements obtained from these studies are presented as “apparent IC₅₀” rather than IC₅₀.

For calcium mobilization assays evaluating receptor activation, A431-CCK2R cells stably transfected with human CCK2R and AR42J cells expressing rat CCK2R were seeded in flat clear bottom black 96-well plates (Corning, Bagnaux-sur-Loing, France), previously coated with poly-D-ornithine (100 µg/mL, 1 h, 37 °C), at densities of 60 000 and 120 000 cells/well, respectively. After 24 h in culture in a 5% CO₂ atmosphere, the cells were rinsed twice with modified HBSS buffer (20 mM HEPES, 0.5 mM MgCl₂, 2.6 mM CaCl₂, 7.7 mM Na₂CO₃, 1.4 mM MgSO₄, 5.3 mM KCl, 138 mM NaCl, 0.1% BSA, 5.5 mM glucose, 2.5 mM probenecid, pH 7.4) (Sigma-Aldrich, Saint-Quentin-Fallavier, France) and loaded (40 min at 37 °C) with the calcium-sensitive dye Fluo-4 AM (ThermoFisher Scientific, Montigny-Le-Bretonneux, France) containing pluronic acid (20% in dimethyl sulfoxide (DMSO)). The cells were then washed twice with modified HBSS, and the effects of graded concentrations of 1–3 and pentagastrin on Ca²⁺ mobilization were measured during 150 s with a FlexStation III fluorometric imaging plate reader (Molecular Devices, Sunnyvale, CA) with an excitation wavelength of 485 nm and an emission wavelength of 525 nm. Briefly, after 18 s recording in basal conditions, 50 µL of graded concentrations of the investigated peptides was added to the incubation medium with a built-in eight-channel pipettor to assess activity. After subtraction of mean

fluorescence background, data were normalized taking as references the amplitudes measured after ejection of medium alone (0%, no self-effect) or 10^{-6} M pentagastrin (100%, maximum response). EC_{50} values were calculated with the Prism 4.0 software using a logistic equation. Results were expressed as mean \pm standard error of the mean (SEM) for at least three independent experiments in triplicate.

Cell Uptake Studies. For internalization experiments, A431-CCK2R and A431-mock cells were seeded at a density of 1.0×10^6 cells per well in six-well plates and grown for 48 h until reaching almost confluence. On the day of the experiment, the cells were washed twice with ice-cold internalization medium supplemented with 1% (v/v) fetal bovine serum. The assay was performed at a final peptide concentration of 0.4 nM in a total volume of 1.5 mL at a temperature of 37 °C three times in triplicate ($n = 3$). Cell uptake was stopped by removal of the medium and rapid rinsing with ice-cold internalization medium (two times) followed by an acid wash (50 mM glycine buffer pH 2.8, 0.1 M NaCl, two times) for 5 min, to remove the membrane-bound radioligand (two times). Finally, the cells were lysed in 2 mL of 1 M NaOH and collected (internalized radioligand fraction). All of the collected fractions (supernatant, surface wash, lysed cells) were measured together with a standard in the γ counter. The radioactivity of the lysed cells was expressed as a percentage of the total radioactivity added (% of internalized radioactivity). The same assays were performed with A431-mock cells for control. Cell internalization of 1–3 was evaluated after ^{111}In -labeling at five different time points for up to 4 h.

Stability Studies in BALB/c Mice. All animal experiments were conducted according to Austrian animal protection laws and with the approval of the Austrian Ministry of Science (BMWF-66.011/0075-WF/V/3b/2016).

Metabolic studies evaluating the stability of the radioligands were carried out in 7- to 8-week-old female BALB/c mice. With the ^{111}In -labeled peptide derivatives, the studies were performed for the time point of 10 min p.i. ($n = 2$). With the ^{177}Lu -labeled peptide derivatives, additional studies were also carried out for the time point of 30 min and 60 min p.i. ($n = 1$ for each time point). To allow monitoring of the metabolites by analytical HPLC, the mice were injected with a higher amount of radioactivity (6–9 MBq indium-111, 30–45 MBq lutetium-177) corresponding to ~ 1 nmol total peptide intravenously through a lateral tail vein. At different time points, the mice were euthanized by cervical dislocation and urine and a blood sample was collected. Liver and kidneys were excised and homogenized in 20 mM HEPES buffer pH 7.3. The amount of intact radioligand and the formation of metabolites was analyzed by analytical HPLC. Prior to injection into the HPLC system, all samples were treated as described for human serum and rat organ homogenate samples.

Biodistribution in BALB/c Nude Mice Bearing A431-CCK2/Mock Xenografts. Biodistribution studies evaluating the tumor uptake of the radiolabeled peptides were performed in 7- to 9-week-old female athymic BALB/c nude mice (Charles River, Sulzfeld, Germany). For the induction of tumor xenografts, 150 μL of DMEM containing 2×10^6 A431-CCK2R and A431-mock cells were injected subcutaneously in the right and left flank of each mouse, respectively. And 10–14 days after injection, tumors reached a medium weight of ~ 0.25 g. The mice were divided into groups of four and injected intravenously *via* a lateral tail vein with 0.2 MBq of ^{111}In -labeled compound (0.02 nmol) and 0.7 and 1.5 MBq of the ^{177}Lu -labeled compound (0.02 and 0.15 nmol). At 4 and 12 h p.i., the mice were sacrificed and the tumors and other tissues (blood, lung, heart, muscle, spleen, intestine, liver, kidneys, stomach, and pancreas) were removed, weighed, and their radioactivity measured in the γ counter together with the rest of the body. Initial biodistribution studies were performed with the three ^{177}Lu -labeled CCK2R-targeting ligands at an injected peptide amount of 20 pmol for the time point of 4 h p.i. From these studies, two peptide analogues were selected to further characterize the biodistribution profile also at a later time point of 12 h p.i. and at a higher injected peptide amount of 150 pmol. Additional animal studies were performed for the ^{111}In -labeled conjugates. Percentage of injected activity per gram tissue (%IA/g), tumor-to-

organ activity ratios, as well as whole body activity were calculated for each sample and statistical analysis using independent two-population *t*-test (significance level $p < 0.05$) was performed using Origin software. For the comparison of more than two groups, data were analyzed using one-way analysis of variance (ANOVA) Holm–Bonferroni-adjusted post hoc analysis (significance level $p < 0.05$) using Microsoft Excel 2010 software (Microsoft Excel 2010, Microsoft Corporation, WA).

■ ASSOCIATED CONTENT

SI Supporting Information

The Supporting Information is available free of charge at <https://pubs.acs.org/doi/10.1021/acs.jmedchem.0c01233>.

UV chromatograms and MS spectra of all of the three synthesized compounds; radiochromatograms after labeling with indium-111 and lutetium-177; radiochromatograms of *in vitro* stability analysis in rat organ homogenates; further data of *in vivo* stability analysis of blood, liver, kidney, and urine of BALB/c mice with the ^{111}In - and ^{177}Lu -labeled peptide analogues; further data regarding biodistribution studies in A431-CCK2R/A431-mock xenografted BALB/c nude mice with [^{177}Lu]Lu-1 and [^{177}Lu]Lu-2; and details for the radioiodination of [Leu 15]gastrin-I (PDF)

Molecular formula strings (CSV)

■ AUTHOR INFORMATION

Corresponding Author

Elisabeth von Guggenberg – Department of Nuclear Medicine, Medical University of Innsbruck, 6020 Innsbruck, Austria; orcid.org/0000-0003-4944-4705; Email: elisabeth.von-guggenberg@i-med.ac.at

Authors

Maximilian Klingler – Department of Nuclear Medicine, Medical University of Innsbruck, 6020 Innsbruck, Austria
Anton A. Hörmann – Department of Nuclear Medicine, Medical University of Innsbruck, 6020 Innsbruck, Austria
Christine Rangger – Department of Nuclear Medicine, Medical University of Innsbruck, 6020 Innsbruck, Austria
Laurence Desrues – INSERM U1239, DC2N, Institute for Research and Innovation in Biomedicine (IRIB), University of Rouen Normandy, 76000 Rouen, France
Hélène Castel – INSERM U1239, DC2N, Institute for Research and Innovation in Biomedicine (IRIB), University of Rouen Normandy, 76000 Rouen, France; orcid.org/0000-0002-8972-5555
Pierrick Gandolfo – INSERM U1239, DC2N, Institute for Research and Innovation in Biomedicine (IRIB), University of Rouen Normandy, 76000 Rouen, France

Complete contact information is available at: <https://pubs.acs.org/doi/10.1021/acs.jmedchem.0c01233>

Author Contributions

The manuscript was written through contributions of all authors. All authors have given approval to the final version of the manuscript.

Funding

This study was financially supported by the Austrian Science Fund (FWF) (project P 27844).

Notes

The authors declare no competing financial interest.

■ ABBREVIATIONS

ACN, acetonitrile; BSA, bovine serum albumin; BOC, *tert*-butyloxycarbonyl; CCK, cholecystokinin; CCK2R, cholecystokinin-2 receptors; DMEM, Dulbecco's modified Eagle's medium; DTPA, diethylenetriaminepentaacetic acid; DOTA, 1,4,7,10-tetraazacyclododecane-1,4,7,10-tetraacetic acid; HATU, *O*-(7-azabenzotriazole-1-yl)-*N,N,N'*-tetramethyluronium hexa-fluorophosphate; HCCA, α -cyano-4-hydroxycinnamic acid; HEPES, 4-(2-hydroxyethyl)-1-piperazineethanesulfonic acid; HOAt, 1-hydroxy-7-aza-benzotriazole; MTC, medullary thyroid carcinoma; MG, minigastrin; (*N*-Me)-Nle, *N*-methyl-norleucine; NMP, *N*-methyl-2-pyrrolidone; RCP, radiochemical purity; RT, room temperature; SPPS, solid-phase peptide synthesis; SPE, solid-phase extraction; TFA, trifluoroacetic acid

■ REFERENCES

- (1) Roosenburg, S.; Laverman, P.; van Delft, F. L.; Boerman, O. C. Radiolabeled CCK/Gastrin Peptides for Imaging and Therapy of CCK2 Receptor-Expressing Tumors. *Amino Acids* **2011**, *41*, 1049–1058.
- (2) Kaloudi, A.; Nock, B. A.; Krenning, E. P.; Maina, T.; De Jong, M. Radiolabeled Gastrin/CCK Analogs in Tumor Diagnosis: Towards Higher Stability and Improved Tumor Targeting. *Q. J. Nucl. Med. Mol. Imaging* **2015**, *59*, 287–302.
- (3) Reubi, J. C.; Schaer, J. C.; Waser, B. Cholecystokinin(CCK)-A and CCK-B/Gastrin Receptors in Human Tumors. *Cancer Res.* **1997**, *57*, 1377–1386.
- (4) Reubi, J. C. Targeting CCK Receptors in Human Cancers. *Curr. Top. Med. Chem.* **2007**, *7*, 1239–1242.
- (5) Sanchez, C.; Escriet, C.; Clerc, P.; Gigoux, V.; Waser, B.; Reubi, J. C.; Fourmy, D. Characterization of a Novel Five-Transmembrane Domain Cholecystokinin-2 Receptor Splice Variant Identified in Human Tumors. *Mol. Cell. Endocrinol.* **2012**, *349*, 170–179.
- (6) Reubi, J. C.; Waser, B. Comcomitant Expression of Several Peptide Receptors in Neuroendocrine Tumours: Molecular Basis for in Vivo Multireceptor Tumour Targeting. *Eur. J. Nucl. Med. Mol. Imaging* **2003**, *30*, 781–793.
- (7) Noble, F.; Wank, S. A.; Crawley, J. N.; Bradwejn, J.; Seroogy, K. B.; Hamon, M.; Roques, B. P. International Union of Pharmacology. XXI. Structure, Distribution, and Functions of Cholecystokinin Receptors. *Pharmacol. Rev.* **1999**, *51*, 745–781.
- (8) Behr, T. M.; Jenner, N.; Behe, M.; Angerstein, C.; Gratz, S.; Raue, F.; Becker, W. Radiolabeled Peptides for Targeting Cholecystokinin-B/Gastrin Receptor-Expressing Tumors. *J. Nucl. Med.* **1999**, *40*, 1029–1044.
- (9) Dufresne, M.; Seva, C.; Fourmy, D. Cholecystokinin and Gastrin Receptors. *Physiol. Rev.* **2006**, *86*, 805–847.
- (10) Aloj, L.; Aurilio, M.; Rinaldi, V.; D'ambrosio, L.; Tesaro, D.; Peitl, P. K.; Maina, T.; Mansi, R.; Von Guggenberg, E.; Joosten, L.; Sosabowski, J. K.; Breeman, W. A. P.; De Blois, E.; Koelewijn, S.; Melis, M.; Waser, B.; Beetschen, K.; Reubi, J. C.; De Jong, M. Comparison of the Binding and Internalization Properties of 12 DOTA-Coupled and 111In-Labelled CCK2/Gastrin Receptor Binding Peptides: A Collaborative Project under COST Action BM0607. *Eur. J. Nucl. Med. Mol. Imaging* **2011**, *38*, 1417–1425.
- (11) Laverman, P.; Joosten, L.; Eek, A.; Roosenburg, S.; Peitl, P. K.; Maina, T.; Mäcke, H.; Aloj, L.; Von Guggenberg, E.; Sosabowski, J. K.; De Jong, M.; Reubi, J. C.; Oyen, W. J. G.; Boerman, O. C. Comparative Biodistribution of 12 111In-Labelled Gastrin/CCK2 Receptor-Targeting Peptides. *Eur. J. Nucl. Med. Mol. Imaging* **2011**, *38*, 1410–1416.
- (12) Ocak, M.; Helbok, A.; Rangger, C.; Peitl, P. K.; Nock, B. A.; Morelli, G.; Eek, A.; Sosabowski, J. K.; Breeman, W. A. P.; Reubi, J. C.; Decristoforo, C. Comparison of Biological Stability and Metabolism of CCK2 Receptor Targeting Peptides, a Collaborative

Project under COST BM0607. *Eur. J. Nucl. Med. Mol. Imaging* **2011**, *38*, 1426–1435.

(13) Béhé, M.; Behr, T. M. Cholecystokinin-B (CCK-B)/Gastrin Receptor Targeting Peptides for Staging and Therapy of Medullary Thyroid Cancer and Other CCK-B Receptor Expressing Malignancies. *Biopolymers* **2002**, *66*, 399–418.

(14) Béhé, M.; Becker, W.; Gotthardt, M.; Angerstein, C.; Behr, T. M. Improved Kinetic Stability of DTPA-DGlu as Compared with Conventional Monofunctional DTPA in Chelating Indium and Yttrium: Preclinical and Initial Clinical Evaluation of Radiometal Labelled Minigastrin Derivatives. *Eur. J. Nucl. Med. Mol. Imaging* **2003**, *30*, 1140–1146.

(15) Behr, T. M.; Jenner, N.; Radetzky, S.; Béhe, M.; Gratz, S.; Yüceken, S.; Raue, F.; Becker, W. Targeting of Cholecystokinin-B/Gastrin Receptors in Vivo: Preclinical and Initial Clinical Evaluation of the Diagnostic and Therapeutic Potential of Radiolabelled Gastrin. *Eur. J. Nucl. Med.* **1998**, *25*, 424–430.

(16) Béhé, M.; Kluge, G.; Becker, W.; Gotthardt, M.; Behr, T. M. Use of Polyglutamic Acids to Reduce Uptake of Radiometal-Labelled Minigastrin in the Kidneys. *J. Nucl. Med.* **2005**, *46*, 1012–1015.

(17) Good, S.; Walter, M. A.; Waser, B.; Wang, X.; Müller-Brand, J.; Béhé, M. P.; Reubi, J. C.; Maecke, H. R. Macrocyclic Chelator-Coupled Gastrin-Based Radiopharmaceuticals for Targeting of Gastrin Receptor-Expressing Tumours. *Eur. J. Nucl. Med. Mol. Imaging* **2008**, *35*, 1868–1877.

(18) von Guggenberg, E.; Dietrich, H.; Skvortsova, I.; Gabriel, M.; Virgolini, I. J.; Decristoforo, C. 99mTc-Labelled HYNIC-Minigastrin with Reduced Kidney Uptake for Targeting of CCK-2 Receptor-Positive Tumours. *Eur. J. Nucl. Med. Mol. Imaging* **2007**, *34*, 1209–1218.

(19) Kolenc-Peitl, P.; Mansi, R.; Tamma, M.; Gmeiner-Stopar, T.; Sollner-Dolenc, M.; Waser, B.; Baum, R. P.; Reubi, J. C.; Maecke, H. R. Highly Improved Metabolic Stability and Pharmacokinetics of Indium-111-DOTA-Gastrin Conjugates for Targeting of the Gastrin Receptor. *J. Med. Chem.* **2011**, *54*, 2602–2609.

(20) Sauter, A. W.; Mansi, R.; Hassiepen, U.; Müller, L.; Panigada, T.; Wiehr, S.; Wild, A.-M.; Geistlich, S.; Béhé, M.; Rottenburger, C.; Wild, D.; Fani, M. Targeting of the Cholecystokinin-2 Receptor with the Minigastrin Analog 177Lu-DOTA-PP-F11N: Does the Use of Protease Inhibitors Further Improve In Vivo Distribution? *J. Nucl. Med.* **2019**, *60*, 393–399.

(21) Kolenc Peitl, P.; Tamma, M.; Kroselj, M.; Braun, F.; Waser, B.; Reubi, J. C.; Sollner Dolenc, M.; Maecke, H. R.; Mansi, R. Stereochemistry of Amino Acid Spacers Determines the Pharmacokinetics of ¹¹¹In-DOTA-Minigastrin Analogues for Targeting the CCK2/Gastrin Receptor. *Bioconjugate Chem.* **2015**, *26*, 1113–1119.

(22) Maina, T.; Konijnenberg, M. W.; KolencPeitl, P.; Garnuszek, P.; Nock, B. A.; Kaloudi, A.; Kroselj, M.; Zaletel, K.; Maecke, H.; Mansi, R.; Erba, P.; von Guggenberg, E.; Hubalewska-Dydejczyk, A.; Mikolajczak, R.; Decristoforo, C. Preclinical Pharmacokinetics, Biodistribution, Radiation Dosimetry and Toxicity Studies Required for Regulatory Approval of a Phase I Clinical Trial with 111In-CP04 in Medullary Thyroid Carcinoma Patients. *Eur. J. Pharm. Sci.* **2016**, *91*, 236–242.

(23) Hubalewska-Dydejczyk, A.; Mikolajczak, R.; Decristoforo, C.; Kolenc-Peitl, P.; Erba, P. A.; Zaletel, K.; Maecke, H.; Maina, T.; Konijnenberg, M.; Garnuszek, P.; Trofimiuk-Müldner, M.; Przybylik-Mazurek, E.; Virgolini, I.; Jong, M.; de Froberg, A. C.; Rangger, C.; Goebel, G.; Scarpa, L.; Glowa, B.; Skórkiewicz, K.; Lezaic, L.; Solnica, B.; Fedak, D.; Gawęda, P.; Sowa-Staszczak, A.; Nock, B. A.; Bergant, D.; Rep, S.; Lenda-Tracz, V. Phase I Clinical Trial Using a Novel CCK2 Receptor-Localizing Radiolabelled Peptide Probe for Personalized Diagnosis and Therapy of Patients with Progressive or Metastatic Medullary Thyroid Carcinoma - Final Results. *Eur. J. Nucl. Med. Mol. Imaging* **2019**, *46*, S339.

(24) Rottenburger, C.; Nicolas, G. P.; McDougall, L.; Kaul, F.; Cachovan, M.; Vija, A. H.; Schibli, R.; Geistlich, S.; Schumann, A.; Rau, T.; Glatz, K.; Behe, M.; Christ, E. R.; Wild, D. Cholecystokinin-2 Receptor Agonist 177Lu-PP-F11N for Radionuclide Therapy of

Medullary Thyroid Carcinoma - Results of the Lumed Phase 0a Study. *J. Nucl. Med.* **2020**, *61*, 520.

(25) Breeman, W. A. P.; Fröberg, A. C.; de Blois, E.; van Gameren, A.; Melis, M.; de Jong, M.; Maina, T.; Nock, B. A.; Erion, J. L.; Mäcke, H. R.; Krenning, E. P. Optimised Labeling, Preclinical and Initial Clinical Aspects of CCK-2 Receptor-Targeting with 3 Radiolabeled Peptides. *Nucl. Med. Biol.* **2008**, *35*, 839–849.

(26) Klingler, M.; Decristoforo, C.; Rangger, C.; Summer, D.; Foster, J.; Sosabowski, J. K.; von Guggenberg, E. Site-Specific Stabilization of Minigastrin Analogs against Enzymatic Degradation for Enhanced Cholecystokinin-2 Receptor Targeting. *Theranostics* **2018**, *8*, 2896–2908.

(27) Klingler, M.; Summer, D.; Rangger, C.; Haubner, R.; Foster, J.; Sosabowski, J.; Decristoforo, C.; Virgolini, I.; von Guggenberg, E. DOTA-MGSS, a New Cholecystokinin-2 Receptor-Targeting Peptide Analog with an Optimized Targeting Profile for Theranostic Use. *J. Nucl. Med.* **2019**, *60*, 1010–1016.

(28) Klingler, M.; Rangger, C.; Summer, D.; Kaeopookum, P.; Decristoforo, C.; von Guggenberg, E. Cholecystokinin-2 Receptor Targeting with Novel C-Terminally Stabilized HYNIC-Minigastrin Analogs Radiolabeled with Technetium-99m. *Pharmaceuticals* **2019**, *12*, No. 13.

(29) Krieger, F.; Fierz, B.; Bieri, O.; Drewello, M.; Kiefhaber, T. Dynamics of Unfolded Polypeptide Chains as Model for the Earliest Steps in Protein Folding. *J. Mol. Biol.* **2003**, *332*, 265–274.

(30) Krieger, F.; Möglich, A.; Kiefhaber, T. Effect of Proline and Glycine Residues on Dynamics and Barriers of Loop Formation in Polypeptide Chains. *J. Am. Chem. Soc.* **2005**, *127*, 3346–3352.

(31) Breeman, W. A.; de Jong, M.; Kwekkeboom, D. J.; Valkema, R.; Bakker, W. H.; Kooij, P. P.; Visser, T. J.; Krenning, E. P. Somatostatin Receptor-Mediated Imaging and Therapy: Basic Science, Current Knowledge, Limitations and Future Perspectives. *Eur. J. Nucl. Med.* **2001**, *28*, 1421–1429.

(32) von Guggenberg, E.; Sallegger, W.; Helbok, A.; Ocak, M.; King, R.; Mather, S. J.; Decristoforo, C. Cyclic Minigastrin Analogues for Gastrin Receptor Scintigraphy with Technetium-99m: Preclinical Evaluation. *J. Med. Chem.* **2009**, *52*, 4786–4793.

(33) Fani, M.; Peitl, P. K.; Velikyan, I. Current Status of Radiopharmaceuticals for the Theranostics of Neuroendocrine Neoplasms. *Pharmaceuticals* **2017**, *10*, No. 30.

(34) Nicolas, G. P.; Morgenstern, A.; Schottelius, M.; Fani, M. New Developments in Peptide Receptor Radionuclide Therapy. *J. Nucl. Med.* **2019**, *60*, 167–171.

(35) Price, E. W.; Orvig, C. Matching Chelators to Radiometals for Radiopharmaceuticals. *Chem. Soc. Rev.* **2014**, *43*, 260–290.

(36) Fani, M.; Maecke, H. R.; Okarvi, S. M. Radiolabeled Peptides: Valuable Tools for the Detection and Treatment of Cancer. *Theranostics* **2012**, *2*, 481–501.

(37) Rangger, C.; Klingler, M.; Balogh, L.; Pöstényi, Z.; Polyak, A.; Pawlak, D.; Mikołajczak, R.; von Guggenberg, E. ¹⁷⁷Lu Labeled Cyclic Minigastrin Analogues with Therapeutic Activity in CCK2R Expressing Tumors: Preclinical Evaluation of a Kit Formulation. *Mol. Pharmaceutics* **2017**, *14*, 3045–3058.

(38) Summer, D.; Rangger, C.; Klingler, M.; Laverman, P.; Franssen, G. M.; Lechner, B. E.; Orasch, T.; Haas, H.; von Guggenberg, E.; Decristoforo, C. Exploiting the Concept of Multivalency with ⁶⁸Ga- and ⁸⁹Zr-Labelled Fusarinine C-Minigastrin Bioconjugates for Targeting CCK2R Expression. *Contrast Media Mol. Imaging* **2018**, *2018*, No. 3171794.

(39) Grob, N. M.; Häussinger, D.; Deupi, X.; Schibli, R.; Behe, M.; Mindt, T. L. Triazolo-Peptidomimetics: Novel Radiolabeled Minigastrin Analogs for Improved Tumor Targeting. *J. Med. Chem.* **2020**, *63*, 4484–4495.

(40) Grob, N. M.; Schmid, S.; Schibli, R.; Behe, M.; Mindt, T. L. Design of Radiolabeled Analogs of Minigastrin by Multiple Amide-to-Triazole Substitutions. *J. Med. Chem.* **2020**, *63*, 4496–4505.

(41) Ocak, M.; Helbok, A.; von Guggenberg, E.; Ozsoy, Y.; Kabasakal, L.; Kremser, L.; Decristoforo, C. Influence of Biological Assay Conditions on Stability Assessment of Radiometal-Labelled

Peptides Exemplified Using a ¹⁷⁷Lu-DOTA-Minigastrin Derivative. *Nucl. Med. Biol.* **2011**, *38*, 171–179.

(42) Mather, S. J.; Mckenzie, A. J.; Sosabowski, J. K.; Morris, T. M.; Ellison, D.; Watson, S. A. Selection of Radiolabeled Gastrin Analogs for Peptide Receptor – Targeted Radionuclide Therapy. *J. Nucl. Med.* **2007**, *48*, 615–622.

(43) Brom, M.; Joosten, L.; Laverman, P.; Oyen, W. J. G.; Béhé, M.; Gotthardt, M.; Boerman, O. C. Preclinical Evaluation of ⁶⁸Ga-DOTA-Minigastrin for the Detection of Cholecystokinin-2/Gastrin Receptor-Positive Tumors. *Mol. Imaging* **2011**, *10*, 144–152.

(44) Konijnenberg, M. W.; Breeman, W. A. P.; de Blois, E.; Chan, H. S.; Boerman, O. C.; Laverman, P.; Kolenc-Peitl, P.; Melis, M.; de Jong, M. Therapeutic Application of CCK2R-Targeting PP-F11: Influence of Particle Range, Activity and Peptide Amount. *EJNMMI Res.* **2014**, *4*, No. 47.

(45) Aloj, L.; Caracò, C.; Panico, M.; Zannetti, A.; Del Vecchio, S.; Tesaro, D.; De Luca, S.; Arra, C.; Pedone, C.; Morelli, G.; Salvatore, M. In Vitro and in Vivo Evaluation of ¹¹¹In-DTPAGlu-G-CCK8 for Cholecystokinin-B Receptor Imaging. *J. Nucl. Med.* **2004**, *45*, 485–494.

(46) Pfister, J.; Summer, D.; Rangger, C.; Petrik, M.; von Guggenberg, E.; Minazzi, P.; Giovenzana, G. B.; Aloj, L.; Decristoforo, C. Influence of a Novel, Versatile Bifunctional Chelator on Theranostic Properties of a Minigastrin Analogue. *EJNMMI Res.* **2015**, *5*, No. 74.